We are IntechOpen,
the world's leading publisher of
Open Access books
Built by scientists, for scientists

6,900
Open access books available

185,000
International authors and editors

200M
Downloads

154
Countries delivered to

Our authors are among the

TOP 1%
most cited scientists

12.2%
Contributors from top 500 universities

BOOK CITATION INDEX
CLARIVATE ANALYTICS
INDEXED

WEB OF SCIENCE™

Selection of our books indexed in the Book Citation Index
in Web of Science™ Core Collection (BKCI)

Interested in publishing with us?
Contact book.department@intechopen.com

Numbers displayed above are based on latest data collected.
For more information visit www.intechopen.com

Uncertainties in Dark Matter Indirect Detection

Katie Auchettl and Csaba Balázs

Additional information is available at the end of the chapter

1. Introduction

Astrophysical observations interpreted in the standard (ΛCDM) cosmological framework indicate that about eighty percent of matter in the Universe is non-luminous. This dark matter poses a major problem for particle physics: no known particle explains its inferred properties. Observations are most consistent with the assumption that dark matter is composed of weakly interacting massive particles. The discovery of these particles is vital to validate the prevailing dark matter paradigm. In this work, we examine the uncertainties affecting the astrophysical discovery of dark matter particles via secondary cosmic ray emission.

Before trying to discover dark matter particles, we should know some of their properties. These properties of dark matter are reconstructed from astrophysical observations, most of which (including the galactic rotational velocities, galactic structure formation, and weak gravitational lensing) indicate that dark matter particles have mass and are present in large numbers around us. Measurements of the cosmic microwave background radiation and the abundance of light elements further suggests that dark matter is not composed of baryonic particles (that is quarks). Since electromagnetic interactions imply light emission, we are led to conclude that dark matter particles may only interact with ordinary matter weakly, either via the standard W and Z bosons, or via an unknown force. Since they are electrically neutral, the simplest assumption is that dark matter particles are their own anti-particles. Their diffuse distribution, inferred from their gravitational effects, indicates that they probably interact weakly with each other. To be present over the observed distance scales, dark matter particles have to be stable on the timescale of the age of the Universe. Lastly, the observed large scale structure indicates that dark matter is cold - its particles are non-relativistic at its present temperature.

Based on the above properties, dark matter particles are being searched for in three major types of experiments. First, since the CERN Large Hadron Collider (LHC) in Geneva was built specifically to explore the electroweak sector of the standard particle model, it is an

obvious place for trying to create dark matter particles. While we are in (almost) full control of this experiment, without knowing the exact mass and interaction strength between ordinary and dark matter we can only hope that the energy and luminosity of the LHC are high enough to produce the latter. Second, because it appears that the Solar System is immersed in a high flux stream of dark matter particles, it is natural to try to detect collisions between them and well shielded nuclei in underground laboratories. These experiments have the potential to probe interactions between dark and ordinary matter even beyond the reach of the LHC. However, these experiments are also limited by the unknown mass, interaction strength, flux and velocity distribution of the dark matter particles. Finally, perhaps the most general and unconstrained way to discover dark matter particles is to find traces of their annihilation or decay products in cosmic rays bombarding Earth.

This last type of experiment is called indirect dark matter detection and it is a sensible way to find dark matter particles if they are either their own anti-particles or the matter-antimatter asymmetry in the dark sector is not pronounced. In this case, via weak interactions, dark matter particles self annihilate into standard ones and create secondary cosmic rays. Alternatively, if dark matter decays into standard particles (with the lifetime of about 10^{26} sec or more) its decay products can contribute to the secondaries. The most promising detection modes are the photon final states or the ones that contribute to anti-matter cosmic rays, such as positrons or anti-protons. In the last few years several anomalies were found in the cosmic positron fluxes by the PAMELA and Fermi-LAT satellites, which could be the first glimpses of dark matter.

However, various factors make indirect detection of dark matter challenging and less straightforward than we would like it to be. First, the immense cosmic ray background originating from ordinary astrophysical sources makes it hard to find the signal contributed by dark matter. Next, in many cases sources of the cosmic ray background are not known or not understood well enough. Finally, an important source of uncertainty and the main subject of our study is the cosmic ray propagation through the galaxy. This propagation is described by the diffusion equation; an equation with many unknown parameters. We review the state of this field of research. We show that using state of the art numerical codes, CPU intensive statistical inference, and the latest cosmic ray observations, the most important of these propagation parameters can be determined with a certain precision. Then we show how to propagate these uncertainties into recent cosmic ray measurements of Fermi-LAT and PAMELA. In the light of these findings we quantify the statistical significance of the present hints of signals in dark matter indirect detection. Finally, we contrast the experimental standing with some of the theoretical dark matter models proposed in the recent literature to explain cosmic ray 'anomalies'.

2. Experimental status of cosmic electrons and positrons

Experiments detecting cosmic rays near Earth have been finding various unexpected deviations from theoretical predictions over the last twenty years. The local flux of high energy positrons is notoriously anomalous as reported by the

- TS [1],
- AMS [2],

- CAPRICE [3],
- MASS [4], and
- HEAT [5, 6]

collaborations. Measurements of the PAMELA satellite stirred great interest by showing an unmistakable rise of the local e^+/e^- fraction, that deviates significantly from theoretical predictions for $E_{e^+} > 10$ GeV [7]. The combined experimental and theoretical uncertainties do not seem to account for such a large excess [8–11].

The summed flux of electrons and positrons also indicates an anomalous excess of observation over theory, as measured by the

- AMS [12],
- PPB-BETS [13], and
- HESS [14, 15]

collaborations. The Fermi Large Area Telescope (LAT) satellite confirmed the excess of the $e^- + e^+$ flux for energies over 100 GeV [16, 17]. The Fermi-LAT results are consistent with those of the PAMELA collaboration, which measured the cosmic ray electron flux up to 625 GeV [18]. To date the Fermi-LAT data are the most precise indication of such an anomaly in the electron-positron spectrum. The Fermi-LAT data differ by several standard deviations from the theoretical calculations encoded in GALPROP by [19].

3. The problem of cosmic ray background calculation

Between 2008 and 2011, of the order of a thousand papers were devoted to explaining the difference between the experimental measurements of Fermi-LAT and PAMELA and theoretical calculations. Speculation ranged from the modification of the cosmic ray propagation through supernova remnants, to dark matter annihilation. A concise summary of this literature with detailed references can be found in [20] and [21].

Before drawing conclusions from the electron-positron anomaly, however, one has to carefully examine the status of the theoretical understanding of Galactic cosmic rays. Unfortunately, even the origin of the cosmic rays is uncertain. The theory describing the propagation of cosmic ray particles from their birthplace through the Milky Way is based on the diffusion-convection model. The quantitative description of propagation is facilitated by the transport equation. This is a partial differential equation for each cosmic ray species which requires fixing the distribution of initial sources and the boundary conditions. Specifying the initial source distribution is a source of significant uncertainty in these calculations. The local cosmic ray fluxes are obtained as the self-consistent solutions of the set of transport equations. Obtaining these solutions is challenging due to the large number of free parameters such as the convection velocities, spatial diffusion coefficients, and momentum loss rates.

In the rest of this chapter we show how to determine those uncertainties of the electron-positron cosmic ray flux that originate from the propagation parameters of the diffusion equation. First we find the set of propagation parameters that the electron-positron flux is most sensitive to. Then we extract the values of these propagation parameters from

cosmic ray data (different from the Fermi-LAT and PAMELA measurements). Based on the values of the propagation parameters most favored by the data we calculate theoretical predictions for the electron-positron fluxes and compare these to Fermi-LAT and PAMELA. By calculating the difference between our predictions and the observed fluxes we are able to isolate the anomalous part of the cosmic e^- and e^+ fluxes.

Similar results have been published in the literature before. However, our results supersede these in two important aspects. First, we show that when analyzed in the framework of the standard propagation model there exists a statistically significant tension between the e^-, e^+ and the rest of the charged cosmic ray fluxes. Second, unlike anyone else before us, we isolate the anomalous contribution within the e^- and e^+ spectrum together with its theoretical uncertainty.

Our analysis uses more charged cosmic ray spectral data points than similar studies before us such as [22]. Unlike us [23] use gamma ray data when extracting the background, however this may bias the analysis since gamma rays originating from anomalous electrons or positrons are not part of the background. Our numerical treatment, similar to that of [24], is more complete than the one of [25–27].

Our statistical analysis can be considered as an extension of [24] since we calculate the e^-, e^+ background with a theoretical uncertainty. Ref. [24] use 76 spectral data points, while we use 219 which gives us a significant edge over their analyses. The parameters that we freely vary are somewhat different from those of [24]. Before we choose the parameter space, we analyzed the sensitivity of the electron and positron spectrum to the parameters to maximize the efficiency of our parameter extraction. Our choice and treatment of the nuisance parameters also differs from [24]. Finally, we use a different scanning technique from the one they use.

4. Cosmic ray propagation through the Galaxy

The propagation of charged particles through the Galaxy can be well described using the diffusion-convection model [28]. This model assumes that the charged particles propagate homogeneously within a defined region of diffusion (similar to the leaky box propagation model), while taking the effects of energy loss into account. The diffusive region is assumed to be a solid flat cylinder defined with a radius R and a half-height of L. Its shape is such that it encloses the Galactic plane which confines charged cosmic rays to the Galactic magnetic fields inside it, while cosmic rays outside are free to stream away. The solar system in this diffusive region is defined in cylindrical coordinates as $\vec{r}_\odot = (8.33\,\text{kpc}, 0\,\text{kpc}, 0\,\text{kpc})$ [29]. The phase-space density $\psi_a(\vec{r}, p, t)$ of a particular cosmic ray species a at time t, Galactic position $\vec{r}$ and with momentum p can be determined by solving the cosmic ray transport equation, which has the general form [30]

$$\frac{\partial \psi_a(\vec{r}, p, t)}{\partial t} = Q_a(\vec{r}, p, t) + \nabla \cdot (D_{xx} \nabla \psi_a - \vec{V}\psi_a)$$

$$+ \frac{\partial}{\partial p}\left(p^2 D_{pp} \frac{\partial}{\partial p} \frac{1}{p^2} \psi_a\right) - \frac{\partial}{\partial p}\left(\dot{p}\psi_a - \frac{p}{3}(\nabla \cdot \vec{V})\psi_a\right) - \frac{1}{\tau_f}\psi_a - \frac{1}{\tau_r}\psi_a. \quad (1)$$

If the time-scale of cosmic ray propagation (which is of the order of 1 Myr at 100 GeV energies) is much longer than the typical time scales of the galactic collapse of dark matter and the variation in the propagation conditions, then one can assume that the steady state condition holds. In this case, the left hand side of equation 1 can be set to zero and the time dependence of all quantities can be dropped. For our analysis we focus on a simplified version of the transport equation which to a first order approximation is sufficient to describe the propagation of electrons, positrons or anti-protons through the Galaxy and their corresponding spectrum at Earth:

$$0 = Q_a(\vec{r}, E) + K(E) \, \nabla^2 \psi_a + \frac{\partial}{\partial E} \Big(b(E) \, \psi_a - K_{EE}(E) \, \psi_a \Big) - \frac{\partial}{\partial z} \left(\mathrm{sign}(z) \, V_C \, \psi_a \right), \quad (2)$$

where E is the energy of the secondary particle species a. To ensure that on the outer surface of the cylinder the cosmic ray density vanishes, boundary conditions are imposed. Similarly, outside of the diffusive region, these boundary condtions allow the particles to freely propagate and escape. This ensures that the modelling is consistent with the physical picture described above. One also imposes the symmetric condition $\partial \psi_a / \partial r (r = 0) = 0$ at $r = 0$. In momentum space, null boundary conditions are imposed.

The transport of cosmic ray species through turbulent magnetic fields, the energy losses experienced by these particles due to Inverse Compton scattering (ICS), synchrotron radiation, Coulomb scattering or bremsstrahlung and their re-acceleration due to their interaction with moving magnetised scattering targets in the Galaxy is defined by the spatial diffusion coefficient $K(E)$, the energy loss rate $b(E)$ and the diffusive re-acceleration coefficient $K_{EE}(E)$ respectively. The effect of Galactic winds propagating vertically from stars in the Galactic disk can be incorporated by defining the convective velocity V_C. The source of the cosmic rays is defined by $Q_a(\vec{r}, E)$ in equation 2, with a standard source term resulting from the annihilation of dark matter which can be written as:

$$Q_a(\vec{r}, E) = \frac{1}{2} \frac{dN_a}{dE} \langle \sigma_a v \rangle_0 \left(\frac{\rho_g(\vec{r})}{m_\chi} \right)^2. \quad (3)$$

Here $\langle \sigma_a v \rangle_0$ corresponds to the thermally averaged annihilation cross section of the relevant species, and $\rho_g(\vec{r})$ is the energy density of dark matter in the Galaxy. The energy distribution of the secondary particle a is defined as dN_a / dE and is normalised per annihilation. This formula applies to self-conjugated annihilating dark matter. In the case of non-self-conjugated dark matter, or of multicomponent dark matter, the quantities in Eq. (3) should be replaced as follows, where an index i denotes a charge state and/or particle species (indeed any particle property, collectively called "component") and $f_i = n_i / n$ is the number fraction of the i-th component:

$$m_\chi \to \sum_i f_i m_i \qquad \text{(mean mass)}, \qquad (4)$$

$$\langle \sigma_a v \rangle \to \sum_{ij} f_i f_j \langle \sigma_{a,ij} v_{ij} \rangle \qquad \text{(mean cross section times relative velocity)}, \quad (5)$$

$$dN_a / dE \to \frac{\sum_{ij} f_i f_j \sigma_{a,ij} v_{ij} \, (dN_{a,ij} / dE)}{\sum_{ij} f_i f_j \sigma_{a,ij} v_{ij}}, \qquad \text{(annihilation spectrum per annihilation)}. \quad (6)$$

The spatial diffusion coefficient $K(E)$ is assumed to have the form

$$K(E) = K_0 \, v^\eta \left(\frac{R}{\text{GeV}} \right)^\delta,$$ (7)

where v is the speed (in units of c) and $R = p/eZ$ is the magnetic rigidity of the cosmic ray particles. Here Z is the effective nuclear charge of the particle and e is the absolute value of its electric charge (if we considered particles other than electrons, positrons, protons or anti-protons then this quantity would be different from 1). At low energies the behaviour of the cosmic rays as they diffuse is controlled using the parameter η. Traditionally one will set $\eta = 1$ but departures from this traditional value to other values (either positive or negative) have been suggested. More detailed treatments allow one to incorporate spatial dependence into the diffusion coefficient ($K(\vec{r}, E)$) and the influence of particle motion on the diffusion of these particles (which leads to anisotropic diffusion).

Synchrotron radiation and Inverse Compton scattering are position dependent phenomena. Synchrotron radiation arises from the interaction of a charged particle with Galactic magnetic fields and thus it depends on the strength of the magnetic field which changes in the Galaxy. Similarly, inverse Compton scattering is dependent on the distribution of background light which varies in the Galaxy. If one neglects this position dependence of energy losses in the Galactic halo and assumes that all energy losses can be described using a relationship that is proportional to E^2 (which is only valid if one neglects energy losses, such as Coulomb losses and bremsstrahlung, and considers only inverse Compton scattering for electrons with relatively low energy - Thomson scattering regime), then the energy loss rate can be parametrized as

$$b(E) = b_0 \, E^2.$$ (8)

In more detailed treatments the spatial dependence associated with the energy loss rate $b(\vec{r}, E)$ would be considered and a more general energy dependence relationship for the energy loss rate would be obtained. Additionally Coulomb losses ($dE/dt \sim$ const) and bremsstrahlung losses ($dE/dt \sim bE$) could also be taken into account. These losses can be calculated using functions dependent on position and energy as well as gas, interstellar radiation and magnetic field distributions [31].

Finally, the diffusive re-acceleration coefficient $K_{\text{EE}}(E)$ is usually parametrized as

$$K_{\text{EE}}(E) = \frac{2}{9} v_{\text{A}}^2 \frac{v^4 \, E^2}{K(E)},$$ (9)

where v_{A} is the Alfvén speed.

A propagator, or Green's function G, is used to describe the evolution of the cosmic ray that originates from a source Q at $\vec{r}_S$ with energy E_S through the diffusive halo and reaches the Earth at point $\vec{r}$ with energy E. This allows the general solution for Eq. (2) to be written as

$$\psi_a(\vec{r}, E) = \int_E^{m_\chi} dE_S \int d^3 r_S \, G(\vec{r}, E; \vec{r}_S, E_S) \, Q_a(\vec{r}_S, E_S).$$ (10)

The differential flux is related to the solution in Eq. (10) via

$$\frac{d\Phi_a}{dE} = \frac{v(E)}{4\pi} \psi_a(\vec{r}, E).$$ (11)

For the propagation of protons or anti-protons in the Galactic halo, additional terms in Eq. (2) should be introduced to account for spallations on the gas in the disk.

5. Statistical framework

We use standard Bayesian parameter inference to determine the statistically favored regions of the propagation parameters $P = \{p_1, ..., p_N\}$ that the electron and positron cosmic ray fluxes are the most sensitive to. For full mathematical details we refer the reader to [21]. Here we only highlight the main concepts used.

Using the experimental data $D = \{d_1, ..., d_M\}$ and their corresponding theoretical predictions $T = \{t_1(P), ..., t_M(P)\}$, as the fuction of the parameters, we construct the likelihood function

$$\mathcal{L}(D|P) = \prod_{i=1}^{M} \frac{1}{\sqrt{2\pi}\sigma_i} \exp(-\chi_i^2(D, P)/2).$$ (12)

Here

$$\chi_i^2(D, P) = \left(\frac{d_i - t_i(P)}{\sigma_i} \right)^2,$$ (13)

and σ_i are the corresponding combined theoretical and experimental uncertainties. Assuming flat priors $\mathcal{P}(P)$, we then construct the posterior probability distribution

$$\mathcal{P}(P|D) = \mathcal{L}(D|P)\mathcal{P}(P)/\mathcal{E}(D).$$ (14)

At this stage the value of the evidence $\mathcal{E}(D)$ is unknown. After integrating over the whole parameter space its value can be recovered as

$$\mathcal{E}(D) = \int \mathcal{L}(D|P)\mathcal{P}(P) \prod_{j=1}^{N} dp_j.$$ (15)

More relevant to our purpose is the adaptive scan of the likelihood function during this integration which will give us the shape of the posterior distribution over the relevant part

of the parameter space (where the likelihood is the highest). Having this shape we can calculate the probability density of a certain theoretical parameter p_i acquiring a given value by marginalization

$$\mathcal{P}(p_i|D) = \int \mathcal{P}(P|D) \prod_{i \neq j=1}^{N} dp_j. \tag{16}$$

Here the integral is carried out over the full range of the parameters. We can also determine Bayesian credibility regions $\mathcal{R}_x$ for each of the parameters:

$$x = \int_{\mathcal{R}_x} \mathcal{P}(p_i|D) \, dp_i. \tag{17}$$

The above relation expresses the fact that x % of the total posterior probability lies within the region $\mathcal{R}_x$.

After examining the electron and positron fluxes for parameter sensitivity we found that the relevant parameters are:

$$P = \{\gamma^{e^-}, \gamma^{nucleus}, \delta_1, \delta_2, D_{0xx}\}. \tag{18}$$

These parameters enter into the diffusion calculation as follows; γ^{e^-} and $\gamma^{nucleus}$ are the primary electron and nucleus injection indices parameterizing an injection spectrum without a break; δ_1 and δ_2 are spatial diffusion coefficients below and above a reference rigidity ρ_0; and D_{0xx} determines the normalization of the spatial diffusion coefficient.

We treat the normalizations of all charged cosmic ray fluxes as theoretical nuisance parameters:

$$P_{nuisance} = \{\Phi_{e-}^0, \Phi_{e+}^0, \Phi_{\bar{p}/p}^0, \Phi_{B/C}^0, \Phi_{(SC+Ti+V)/Fe}^0, \Phi_{Be-10/Be-9}^0\}. \tag{19}$$

We discuss other statistical and numerical issues, such as the choice of priors, the systematic uncertainties, sampling and convergence, in detail in [21].

6. Experimental data used in this analysis

In our statistical analysis we use 219 of the most recent data points corresponding to five different types of cosmic ray experiment. A majority of these data points (114 in total) come from electron-positron related experiments while the other 105 are made up of Boron/Carbon, anti-proton/proton and (Sc+Ti+V)/Fe and Be-10/Be-9 cosmic ray flux measurements. If any of the energy ranges of the experiments overlap, the most recent experimental data point was chosen in that energy range.

There are three main experiments that have measured electrons and positrons over different decades of energy. These experiments include AMS by [12], Fermi-LAT by [17] and HESS by

[14, 15]. The AMS collaboration reported an excess in positrons with energies greater than 10 GeV [12], while the HESS collaboration measured a significant steepening of the electron plus photon spectrum above one TeV as measured by HESS's atmospheric Cherenkov telescope (ACT). Using the Large Area Telescope (LAT) on the Fermi Satellite, the Fermi-LAT collaboration released a high precision measurement of the $e^+ + e^-$ spectrum for energies from 7 GeV to 1 TeV [17], extending the energy range of their previously published results. We defined our $e^+ + e^-$ spectrum by using data from these three experiments. The PAMELA collaboration recently released their measurement of the e^- only spectrum [18] confirming the behaviour of the $e^+ + e^-$ spectrum as measured by Fermi-LAT. The energy ranges that these data points were selected over are listed in Table 1.

Measured flux	Experiment	Energy (GeV)	Number of data points
$e^+ + e^-$	AMS [12]	0.60 - 0.91	3
	Fermi-LAT [17]	7.05 - 886	47
	HESS [14, 15]	918 - 3480	9
$e^+/(e^+ + e^-)$	PAMELA [32]	1.65 - 82.40	16
e^-	PAMELA [18]	1.11 - 491.4	39
anti-proton/proton	PAMELA [33]	0.28 - 129	23
Boron/Carbon	IMP8 [34]	0.03 - 0.11	7
	ISEE3 [35]	0.12 - 0.18	6
	[36]	0.30 - 0.50	2
	HEAO3 [37]	0.62 - 0.99	3
	PAMELA [38]	1.24 - 72.36	8
	CREAM [39]	91 - 1433	3
(Sc+Ti+V)/Fe	ACE [40]	0.14 - 35	20
	SANRIKU [41]	46 - 460	6
Be-10/Be-9	[42]	0.003 - 0.029	3
	[43]	0.034 - 0.034	1
	[42]	0.06 - 0.06	1
	ISOMAX98 [44]	0.08 - 0.08	1
	ACE-CRIS [45]	0.11 - 0.11	1
	ACE [46]	0.13 - 0.13	1
	AMS-02 [47]	0.15 - 9.03	15

Table 1. In this table we have listed the cosmic ray experiments and the energy ranges of the corresponding data points that we selected for our analysis. There are two sets of cosmic ray data listed in this table. Electron positron flux related experiments make up the first five lines of the table, while all other experiments make up the rest of the table. On these two sets of data, we perform a Bayesian analysis to highlight the tension between the two sets of data.

Apart from measuring the electron positron sum, collaborations such as PAMELA have measured the differential positron fraction $e^+/(e^+ + e^-)$ between energies of 1.5 and 100 GeV [7]. If one assumes that all secondary positrons are produced during the propagation of cosmic rays in the Galaxy, one would expect the positron fraction to decrease, however, the observed fraction increases for energies greater than 10 GeV.

How primary and secondary cosmic rays are produced and transported throughout the Galaxy can be studied by using cosmic-ray particles such as anti-protons. One requires a

large number of measurements with good statistics over a large energy range to produce detailed anti-proton spectra for study. Anti-proton spectra obtained from previous balloon borne experiments such as CAPRISE98 [3] and HEAT [48] had very low statistics, but recently the PAMELA satellite experiment [33] released a high-quality measurement of the anti-proton/proton flux ratio for an energy range of 1-100 GeV. This spectrum confirmed the behaviour of the anti-proton/proton ratio as observed by previous experiments.

Additionally one can use stable secondary to primary cosmic ray ratios such as Boron/Carbon and (Sc+Ti+V)/Fe ratio to study the variation experienced by cosmic rays as they propagate through the Galaxy. These ratios are particularly sensitive to the properties of cosmic ray propagation as the element in the numerator is produced by a different mechanism to the element that defines the denominator. Primary cosmic rays are produced by the original source of the cosmic rays such as a supernova remnant, while the secondary cosmic rays are generated by the interaction of their primaries with the interstellar medium [49]. Ratios that are defined by a numerator and denominator which are produced by the same mechanism, such as a primary/primary or a secondary/secondary cosmic ray ratio, have a low sensitivity to any variation in the propagation parameters. Analysing Galactic Boron/Carbon and (Sc+Ti+V)/Fe ratios allows one to determine the amount of interstellar material transversed by the primary cosmic ray and its energy dependence [49].

Unstable isotopes such as Beryllium-10/Beryllium-9 are also beneficial to analyse as they produce a constraint on the time it takes for a cosmic ray to propagate through the Galaxy [50]. Various experiments such as ISOMAX98 [44], ACE-CRIS [45], ACE [46] and AMS-02 [47] have all measured Be-10/Be-9 data with varying statistics.

In Table 1 we state over what energy range and from which experiment we selected the data points that define our spectrum of anti-proton/proton, Boron/Carbon, (Sc+Ti+V)/Fe and Be-10/Be-9 ratio.

For energies below E < 10 GeV, solar magnetic and coronal activities perturb the low energy part of the cosmic ray spectrum. This is called solar modulation and has an important role in determining the observed spectral shape(s) of cosmic rays measured at earth [51, 52]. Solar modulation is accounted for in GALPROP by using a force field approximation. It should be noted that this is an approximation and does not include important influences such as the structure of the heliospheric magnetic field. To incorporate these effects into our analysis we vary the value of the modulation potential in GALPROP. Following Gast & Schael (2009), we also assume that the positively and negatively charged cosmic rays are modulated differently by solar activities (charge-sign dependent modulation). This charge dependent modulation has a significant effect on positrons and its effect on the anti-proton/proton ratio can be comparable to the experiment's statistical uncertainties. The modulation effect on heavy nuclei such as B, C, Sc, Ti, V, Fe and Be is mild even though these nuclei have a higher positive charge compared to the proton. The reason for this is that the modulation potential is proportional to the charge-to-mass ratio and these heavy nuclei have a much lower charge-to-mass ratio than the proton therefore the effect is minute. Regardless, as we use the ratio of their fluxes, most of the effect of solar modulation on these nuclei is cancelled, thus we can safely absorb this modulation effect into the systematic uncertainties of the experiment. To be able to compare experimental data we set the modulation potential in GALPROP for positrons (electrons) to the value determined by Gast & Schael (2009), $\phi+ = 442(2)$ MeV. Previous work by Usoskin et al. (2011) showed that the time dependence of the
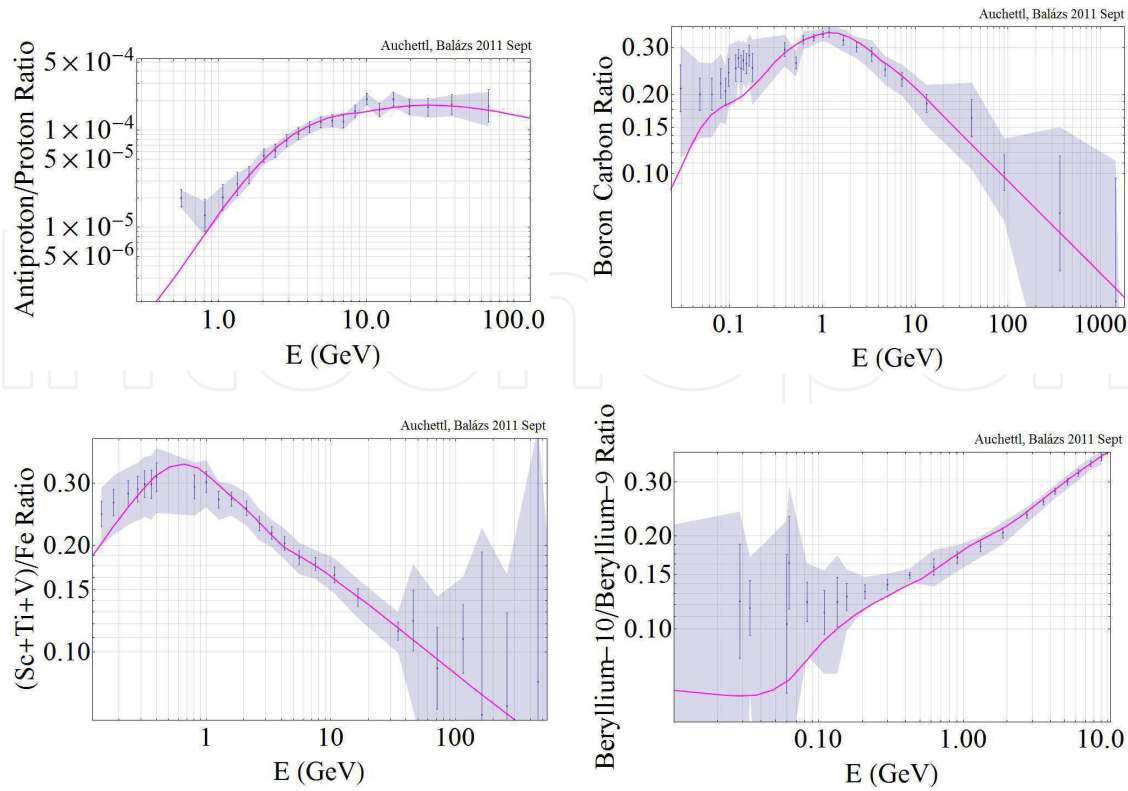
Figure 1. Best fit curves plotted against non-electron-positron related data. These curves were calculated using the most probable parameter values obtained from the peak values of the posterior probabilities (inferred from $\bar{p}/p$, B/C, (Sc+Ti+V)/Fe and Be data) shown in red in Fig. 2. The best fit curves pass through the estimated systematic error bands, shown in gray.

solar modulation potential was not substantial over the period of PAMELA's data taking, and approximately the same average value for the potential can be used for Fermi-LAT.

7. Results

7.1. The presence or absence of a cosmic ray anomaly

There has been a plethora of experiments which have hinted at the existence of an anomaly in the electron-positron spectrum. The most notable measurements are the Fermi-LAT electron positron sum and the PAMELA positron fraction. Ref. [53] and [24] have all questioned the reality of the anomaly in the PAMELA and Fermi-LAT data as well as the absence of an anomaly in the anti-proton flux. Ref. [24] suggested that one requires only to readjust the diffusion parameters that define the propagation model as encoded in GALPROP to reproduce the Fermi-LAT data. This conclusion is highlighted clearly in figure 8 of [24], where their propagation model obtained from the best fit to 76 cosmic ray spectral data points agrees well with the Fermi-LAT data. Interestingly, the corresponding positron fraction obtained from their best fit does not agree with the PAMELA data, indicating that one cannot fit the PAMELA data by simply adjusting the parameters of the propagation model. This indicates to us that the anomaly observed in cosmic electron-positron data is real and rather than adjusting the propagation parameters, one has to perform a detailed investigation of its existence and characteristics.

One of our important results is that just by adjusting the parameters in Eq.(18) and (19) it is possible to generate a theoretical prediction which is fully consistent with the Fermi-LAT $e^- + e^+$ flux measurement. Similarly, we found that both the PAMELA positron fraction and the electron flux can be reproduced by theory. This means that the theory has enough flexibility to accommodate the experimentally measured fluxes.

If one assumes that all types of cosmic ray data (electron-positron related and non-electron-positron related) can be described well using a single set of propagation parameters it quickly becomes obvious that one cannot fit the data simultaneously. To analyse this behaviour, we first divided the cosmic ray data listed in table 1 into two groups: electron and/or positron fluxes as measured by AMS, Fermi, HESS and PAMELA and non-electron and/or positron fluxes such as anti-proton/proton, Boron/Carbon, (Sc+Ti+V)/Fe, Be-10/Be-9. We then attempted to fit only the second group of cosmic ray data, that is, excluding the electron-positron related data. We obtain a χ^2 per degree of freedom of 0.34 from this fit and as a consequence the corresponding best fit curves each pass through all the estimated systematic error bands shown in grey in Fig. 1. When we apply the best-fit parameters to the electron and/or positron flux data, however, we obtain a χ^2 per degree of freedom of 24. Similarly, when we do the converse, i.e. find the best-fit propagation parameters using only the electron-positron related flux, we obtain an excellent χ^2 per degree of freedom of 1.0, but the best-fit parameters gave a larger χ^2 per degree of freedom (3.1) for the non-electron-positron data. As we have a large number (105) of data points the deviations observed between these two sets of data is significant which signals statistically significant tension between electron-positron and non-electron-positron measurements. These results support the conclusion highlighted in Fig. 7 and 8 of [24], that one requires something more than simply adjusting the propagation parameters to accommodate for the cosmic ray anomaly.

This tension between the electron-positron and non-electron-positron measurements was further investigated by performing an independent Bayesian analysis on the two groups of data. This allows us to extract the values of the propagation parameters as preferred by the different sets of data. Interestingly, one can derive information about the propagation parameters of the electron-positron related data from the non-electron-positron related data. This arises due to a number of reasons. Firstly, the value of some propagation parameters such as D_{0xx} is highly dependent on the species that one is modelling the propagation of. Secondly, to model the propagation of cosmic rays one uses the transport equation (equation 1). In this equation a large number of processes, including nuclear fragmentation and decay, are incorporated, which directly affects the predicted secondary electron-positron flux. Thirdly, as the energy density of cosmic rays is comparable to the energy density of the interstellar radiation field and the local magnetic field, different cosmic ray species will influence the dynamics of each species non-negligibly.

As a consequence, even if no electron-positron related data is used in our fit one can still constrain some of the propagation parameters of the electron-positron data. Unfortunately this method does not constrain the value of injection indices sufficiently, so in order to fix these parameters we have to include a minimal amount of information about the electron-positron related fluxes in our analysis. We selected data points from the $e^- + e^+$ spectrum for four reasons: (1) these points cover the largest energy range; (2) before setting out to find the optimal parameter value, within uncertainties the end points of the $e^- + e^+$ spectrum agree with theoretical predictions; (3) for low energies the effect of
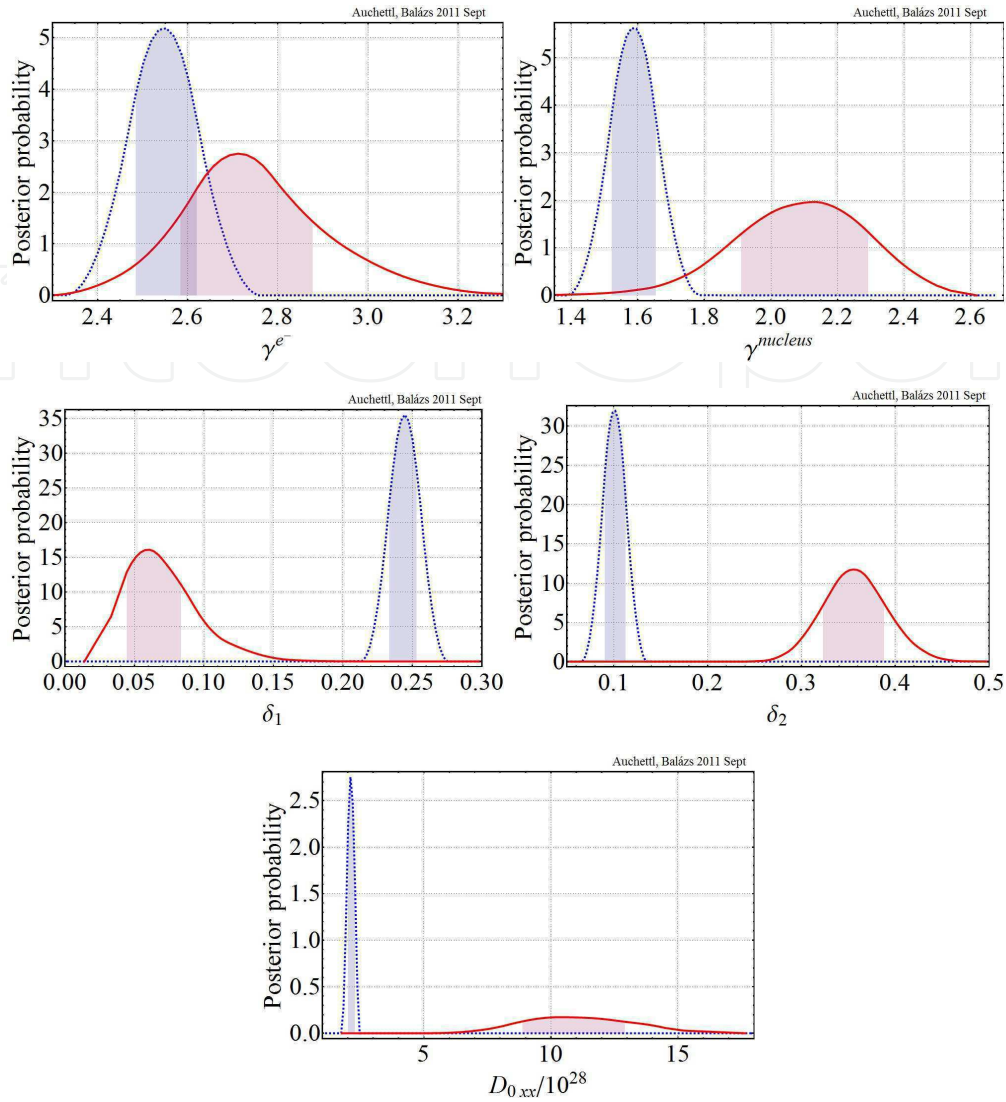
Figure 2. Marginalized posterior probability distributions of propagation parameters listed in Eq.(18). The likelihood functions containing electron and/or positron flux data are plotted as blue dashed lines while the likelihood functions for the rest of the comic ray data are plotted as solid red lines. The 68 % credibility regions are highlighted by the shaded areas of the posteriors. In the lower three frames it is evident that there exists a statistically significant tension between the electron-positron data and the rest.

solar modulation on this data is minor; and (4) the theoretical prediction for the $e^- + e^+$ is insensitive to the value of the propagation parameter for mid-range energies (this is highlighted by the distinct bow-tie shape of the theoretical uncertainty band).

In addition to using non-$e^{\pm}$ related data points (i.e. $\bar{p}/p$, B/C, (Sc+Ti+V)/Fe and Be data), we also selected four $e^{\pm}$ related data points to use in our analysis. This included the lowest energy data point from AMS, the highest energy data point from HESS and the 19.40 GeV and 29.20 GeV data points of Fermi-LAT. We checked that this selection of $e^{\pm}$ related data points does not bias the final conclusion and the results that we obtained with this selection are robust.

In figure 2 we have plotted the marginalized posterior probability densities of our selected propagation parameters as obtained by completing a Bayesian analysis on the two sets

of data. The blue dashed curve represents the likelihood functions generated for the electron-positron related data (AMS, Fermi-LAT, HESS, and PAMELA), while the red solid curves represent the likelihood functions obtained for the rest of the cosmic ray data (anti-proton/proton, Boron/Carbon, (Sc+Ti+V)/Fe, Be-10/Be-9) listed in table 1. The 68% credibility regions of the likelihood functions are highlighted by the shaded areas of figure 2 and table 2 lists the numerical values of these credibility regions as well as the best-fit values of each propagation parameter. By looking at figure 2 it is obvious that the electron-positron related data and the non-electron-positron related data are inconsistent with the hypothesis that the model of cosmic ray propagation and/or the sources encoded in GALPROP provide a sufficient theoretical description.

parameter	Fit for the $e^{\pm}$ related data		Fit for the rest of the data	
	best fit value	68% Cr range	best fit value	68% Cr range
γ^{e^-}	2.55	{2.45, 2.60}	2.71	{2.54, 2.92}
$\gamma^{nucleus}$	1.60	{1.51, 1.69}	2.10	{1.88, 2.92}
δ_1	0.24	{0.23, 0.26}	0.06	{0.04, 0.08}
δ_2	0.10	{0.08, 0.12}	0.35	{0.32, 0.39}
D_{0xx} [$\times 10^{28}$]	2.17	{1.85, 2.19}	11.49	{8.86,13.48}

Table 2. Best fit values of the propagation parameters and their 68 % credibility ranges. Numerical values are shown for both fits: including the electron-positron related cosmic ray data only, and including the rest of the data.

For the posterior densities of the electron and nucleus injection indices γ^{e^-} and $\gamma^{nucleus}$ shown in the first two frames of figure 2, there is a mild but tolerable tension between the two data sets. In the final three frames of figure 2 the posterior densities for δ_1, δ_2 and D_{0xx} are shown. These frames indicate a statistically significant tension between the two sets of data as the 68 % credibility regions of each set for the two spatial diffusion coefficients δ_1 and δ_2, as well as D_{0xx} do not overlap each other. Although not shown it is easily extrapolated that not even the 99% credibility regions of these posteriors will overlap. As a consequence we can conclude that if one adjusts the values of the cosmic ray parameters, one can indeed obtain a good fit for either the electron-positron related data or to the rest of the data individually, however, you cannot obtain a good fit for both sets of data simultaneously.

This tension can be interpreted to mean that the data measured by the PAMELA and Fermi-LAT collaborations is affected by new physics that is unaccounted for by the propagation model and/or cosmic ray sources encoded in GALPROP. Based on simple theoretical arguments, the observed behaviour of the PAMELA positron fraction is unexpected. If one attempts to fit this data by simply adjusting the value of the propagation parameters this will lead to a bad fit of the non-electron-positron related data. One also expects that the anomaly in the PAMELA $e^+/(e^+ + e^-)$ would also produce an observable anomaly in other electron-positron related data such as the Fermi-LAT $e^+ + e^-$ and the PAMELA e^- spectra. This conclusion agrees with the argument of [24] that "secondary positron production in the general ISM is not capable of producing an abundance that rises with energy".

The observed tension in our data is dramatically increased when one incorporates the recently released PAMELA e^- flux [18] in our electron-positron related data. For consistency we checked the result that we would obtain if we excluded this new electron flux data into our

analysis. We noticed that the tension we observe is significantly milder if it is not included. This, and the effect of using a larger amount of data compared to previous studies, suggests why the tension we observe was not detected by authors such as [24].

7.2. The size of the anomaly

As we conclude that new physics is buried within the electron-positron fluxes, we now attempt to extract from the data the size of this new physics signal. Assuming that the new physics affects only the electron-positron fluxes but its influence on the rest of the cosmic ray data is negligible, we can determine the central value and credibility regions of the cosmic ray propagation parameters from the unbiased data: anti-proton/proton, Boron/Carbon, (Sc+Ti+V)/Fe, Be-10/Be-9 to generate a background prediction for all cosmic ray data including the electron-positron fluxes. Once we calculate the theoretical background prediction we can subtract this background from the electron-positron data and determine if a statistically significant signal can be extracted.

To do this we calculate the prediction for the PAMELA and Fermi-LAT electron-positron fluxes by using the central values of the propagation parameters determined using $\bar{p}/p$, B/C, (Sc+Ti+V)/Fe, Be-10/Be-9. Then using all the scanned values of all five propagation parameters lying within the 68 % credibility region we generate a 1-σ uncertainty band for the background around this central value. In figure 3 we overlay the uncertainty background in gray over the Fermi-LAT electron+positron and the PAMELA electron and positron fraction fluxes. For the Fermi-LAT and PAMELA e^- the statistical and systematic uncertainties were combined in quadrature, while as the PAMELA $e^+/(e^+ + e^-)$ only had statistical uncertainties, we scaled these uncertainties using $\tau = 0.2$ to produce the experimental error bands. The magenta bands correspond to our background predictions, while the green dashed lines and band correspond respectively to the central value and the 1-σ uncertainty of the calculated anomaly.

In figure 3 one can see that our background prediction deviates from the data at energies below ≈ 10 GeV and above 100 GeV. For this analysis we focus on the deviation between the background and the data for energies greater than 100 GeV, while for the deviation observed at low energies we leave this to future research, but we note that this deviation could arise from inadequacies of the propagation model. Based on our background prediction we obtain a weak but statistically significant anomaly signal which we interpret as the presence of a new physics in the Fermi-LAT electron+positron flux. A similar conclusion can be drawn about the PAMELA positron fraction when taking the difference between the central values of the data and the background, but due to sizeable uncertainties of the PAMELA measurement we cannot claim a statistically significant deviation. [1]

To determine the size of the new physics signal in the electron positron data we subtract the central value of the corresponding background prediction from the central value of the data. The 1-σ uncertainty band of the signal is obtained by combining the experimental

---

[1] The Fermi-LAT collaboration recently presented a preliminary measurement of the positron fraction [54] which confirmed the results of PAMELA. At first glance this measurement appears to have smaller systematic uncertainties than that of PAMELA. If the officially published Fermi-LAT measurement has systematic errors of approximately the same size as the statistical errors of PAMELA then the data will also deviate from our background unveiling an anomalous signal in the positron fraction.
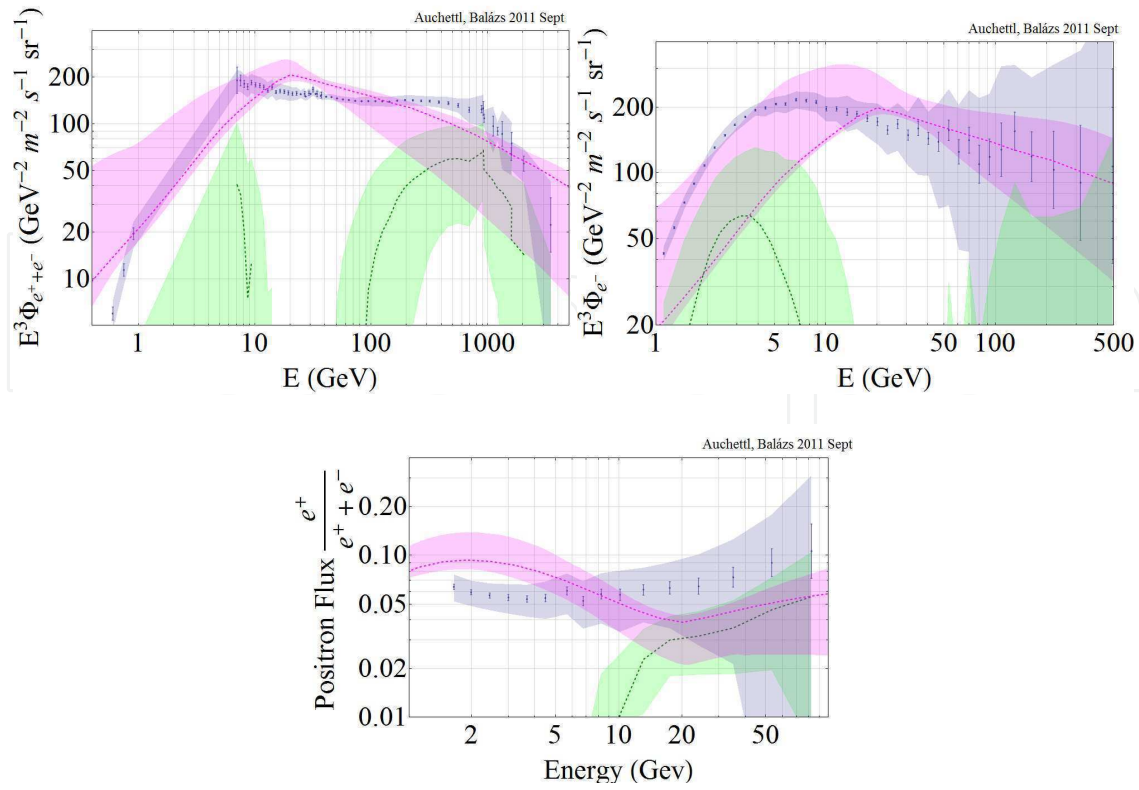
Figure 3. The anomalous signal we extracted for various electron-positron fluxes. The green dotted curves (marking the central values) and bands (showing 68 % credible intervals) correspond to the extracted size of the anomaly. The data points correspond to the spectra measured by Fermi-LAT and PAMELA. Combined statistical and systematic uncertainties are shown (by the gray bands) for Fermi-LAT and PAMELA e^-, while ($\tau = 0.2$) scaled statistical uncertainties are shown for PAMELA $e^+/(e^+ + e^-)$. Overlaid in magenta is our background prediction (central value curve and 68 % credible intervals).

and background uncertainties quadratically. In Fig. 3 the results for the electron-positron anomaly are shown. Based on our background predictions, we obtain a non-vanishing anomalous signal for the Fermi-LAT $e^+ + e^-$ flux, while for the PAMELA data we cannot claim the presence of a statistically significant anomaly due to the large uncertainties of the data.

7.3. The source of the anomaly

Since the publication of the PAMELA positron fraction [7], there have been numerous publications that have speculated on the origin of the discrepancy between the theoretical prediction of electron-positron spectra and the experimental data. Based on the available evidence we can only postulate on the origin of this deviation. An obvious guess would be that the model used to describe the propagation of electrons and positrons in our Galaxy is insufficient in some respect, which if correct would mean that there exists no anomalous signal in the data. One such reasonable effect which is not incorporated in the two dimensional GALPROP calculation is the spectral hardening of cosmic ray spectra due to the presence of non-steady sources. To confirm these possibilities it would be an interesting exercise to repeat our analysis using different calculation tools such as DRAGON by [55], USINE by [56], PPPC4DMID by [57] or the code of [58].

If one assumes that the propagation model satisfactorily describes the propagation of cosmic rays through our Galaxy it is only natural to suspect that local effects are modifying the distribution of electrons and positrons. The lack of sources included in the GALPROP calculation seem to confirm this suspicion. There have been a plethora of papers that account for this anomaly by proposing various new sources of cosmic rays. There are two major categories of new cosmic ray sources that have been proposed. The first involves known astrophysical objects with uncertain parameters such as supernova remnants, pulsars, or various other objects in the Galactic centre, while the second involves more exotic astronomical and/or particle physics phenomena such as dark matter. Literature discussing these cases is extensively cited by [21].

For energies greater than 100 GeV, energy losses such as inverse Compton scattering of interstellar dust and cosmic microwave background light or synchrotron radiation become important. These effects result in a relatively short lifetime of the electron and positron while simultaneously this causes a decrease in the intensity of these particles as energy increases. As a result it is hypothesised that a large number of the electrons and positrons detected at Earth with an energy above 100 GeV come from individual sources within a few kilo-parsecs of Earth [51, 52]. Random fluctuations in the injection spectrum and spatial distribution of these nearby sources can produce detectable differences between the predicted background and the most energetic part of the observed electron and positron spectrum. This deviation could indicate the presence of new physics arising from either an astrophysical object(s) or dark matter.

If the size of the anomalous signal can be isolated from the experimental data then, regardless of the origin of the anomaly, the source will have to produce a signal with those characteristics. In Fig. 4 we compare our extracted signal to a few randomly selected attempts from the literature to match this anomaly. The first frame features the spectrum of electrons and positrons unaccounted for from local supernovae as calculated by [59] . The top right frame shows the contribution from additional primary cosmic ray sources such as pulsars or annihilation of particle dark matter as calculated by [52]. The bottom left frame contains the predictions of [60] for anomalous electron-positron sources from dark matter annihilations, while the last frame shows the dark matter annihilation contributions calculated by [61].

If the theoretical uncertainty of a new cosmic ray source and its contribution to cosmic ray measurements at Earth is unknown it can be difficult to draw any conclusion about its contribution to our isolated signal. In the case where the theoretical uncertainty of a new cosmic ray source is known it usually tends to be of significant size that it can prevent us from judging whether it is a valid explanation of our signal. Regardless, we can select a few scenarios that are more likely to be favoured than some others based on the present amount of information we have obtained from our analysis. With more data it will be possible to reduce the size of the uncertainty of our signal, while with more detailed calculations we can produce a more precise prediction of the cosmic ray spectrum as measured at Earth. This may enable the various suggestions of the source of the electron-positron anomaly to be confirmed or ruled out.
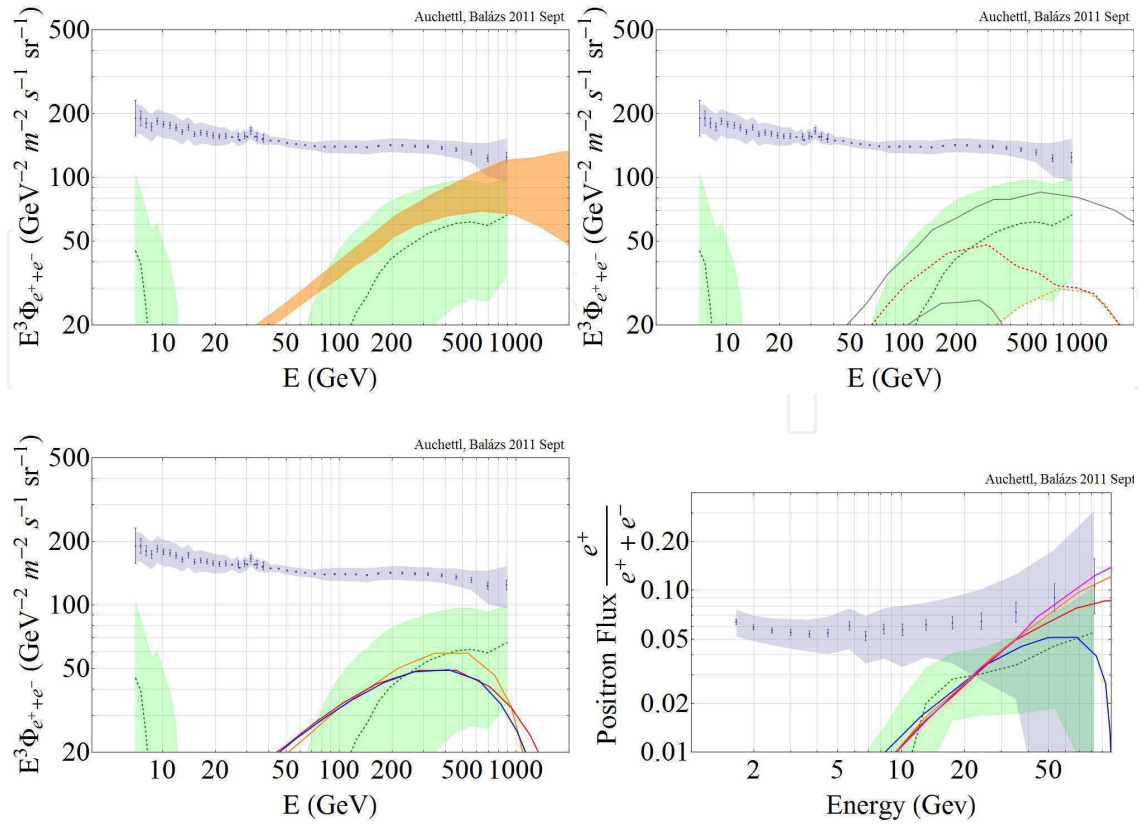
Figure 4. Comparing the detected cosmic ray flux (data points and gray band) and the signal extracted in this work (green dotted curve and band) to potential explanations of the electron-positron cosmic ray anomaly (solid curves). The various theoretical predictions come from [59], [52], [60] and [61]. Currently the comparison is fairly inconclusive but with more data it will be possible to shrink the uncertainty in the determination of the signal. Then various suggestions can be confirmed or ruled out.

8. Conclusions

Motivated by the possibility of new physics contributing to the measurements of PAMELA and Fermi-LAT, we subjected a wide range of cosmic ray observations to a Bayesian likelihood analysis. In the context of the propagation model coded in GALPROP, we found a significant tension between the $e^- \backslash e^+$ related data and the rest of the cosmic ray fluxes. This tension can be interpreted as the failure of the model to describe all the data simultaneously or as the effect of a missing source component.

Since the PAMELA and Fermi-LAT data are suspected to contain a component unaccounted for in GALPROP, we extracted the preferred values of the cosmic ray propagation parameters from the non-electron-positron related measurements. Based on these parameter values we calculated background predictions, with uncertainties, for PAMELA and Fermi-LAT. We found a deviation between the PAMELA and Fermi-LAT data and the predicted background even when uncertainties, including systematics, were taken into account. Interpreting this as an indication of new physics we subtracted the background from the data isolating the size of the anomalous component.

The signal of new physics in the electron+positron spectrum was found to be non-vanishing within the calculated uncertainties. Thus the use of 219 cosmic ray spectral data points within the Bayesian framework allowed us to confirm the existence of new physics effects in

the electron+positron flux in a model independent fashion. Using the statistical techniques we were able to extract the size, shape and uncertainty of the anomalous contribution in the $e^- + e^+$ cosmic ray spectrum. We briefly compared the extracted signal to some theoretical results predicting such an anomaly.

Author details

Katie Auchettl and Csaba Balázs

Monash University, Australia

References

[1] R. L. Golden et al. Observations of cosmic ray electrons and positrons using an imaging calorimeter. *Astrophys. J.*, 436:769–775, 1994.

[2] J. Alcaraz et al. Leptons in near earth orbit. *Phys. Lett.*, B484:10–22, 2000.

[3] M. Boezio et al. The cosmic-ray anti-proton flux between 3-GeV and 49- GeV. *Astrophys. J.*, 561:787–799, 2001.

[4] C. Grimani et al. Measurements of the absolute energy spectra of cosmic-ray positrons and electrons above 7-GeV. *Astron. Astrophys.*, 392:287–294, 2002.

[5] S. W. Barwick et al. Measurements of the cosmic-ray positron fraction from 1- GeV to 50-GeV. *Astrophys. J.*, 482:L191–L194, 1997.

[6] J. J. Beatty et al. New measurement of the cosmic-ray positron fraction from 5-GeV to 15-GeV. *Phys. Rev. Lett.*, 93:241102, 2004.

[7] Oscar Adriani et al. An anomalous positron abundance in cosmic rays with energies 1.5-100 GeV. *Nature*, 458:607–609, 2009.

[8] T. Delahaye et al. Galactic secondary positron flux at the Earth. *Astron. Astrophys.*, 501:821–833, 2009.

[9] T. Delahaye, J. Lavalle, R. Lineros, F. Donato, and N. Fornengo. Galactic electrons and positrons at the Earth:new estimate of the primary and secondary fluxes. *Astron. Astrophys.*, 524:A51, 2010.

[10] Philipp Mertsch. Cosmic ray backgrounds for dark matter indirect detection. *arXiv:1012.4239*, 2010.

[11] Timur Delahaye, Fiasson Armand, Martin Pohl, and Pierre Salati. The GeV-TeV Galactic gamma-ray diffuse emission I. Uncertainties in the predictions of the hadronic component. *arXiv:1102.0744*, 2011.

[12] M. Aguilar et al. The Alpha Magnetic Spectrometer (AMS) on the International Space Station. I: Results from the test flight on the space shuttle. *Phys. Rept.*, 366:331–405, 2002.

[13] S. Torii et al. High-energy electron observations by PPB-BETS flight in Antarctica. *arXiv:0809.0760*, 2008.

[14] F. Aharonian et al. The energy spectrum of cosmic-ray electrons at TeV energies. *Phys. Rev. Lett.*, 101:261104, 2008.

[15] F. Aharonian et al. Probing the ATIC peak in the cosmic-ray electron spectrum with H.E.S.S. *Astron. Astrophys.*, 508:561, 2009.

[16] Aous A. Abdo et al. Measurement of the Cosmic Ray e+ plus e- spectrum from 20 GeV to 1 TeV with the Fermi Large Area Telescope. *Phys. Rev. Lett.*, 102:181101, 2009.

[17] M. Ackermann et al. Fermi LAT observations of cosmic-ray electrons from 7 GeV to 1 TeV. *Phys. Rev.*, D82:092004, 2010.

[18] O. Adriani et al. The cosmic-ray electron flux measured by the PAMELA experiment between 1 and 625 GeV. *Phys. Rev. Lett.*, 106(20):201101, 2011.

[19] A. W. Strong and I. V. Moskalenko. Propagation of cosmic-ray nucleons in the Galaxy. *Astrophys. J.*, 509:212–228, 1998.

[20] Pasquale D. Serpico. Astrophysical models for the origin of the positron 'excess', 2011.

[21] Katie Auchettl and Csaba Balazs. Extracting the size of the cosmic electron-positron anomaly. *Astrophys.J.*, 749:184, 2012.

[22] A. Putze, L. Derome, and D. Maurin. A Markov Chain Monte Carlo technique to sample transport and source parameters of Galactic cosmic rays. II. Results for the diffusion model combining B/C and radioactive nuclei. *Astronomy and Astrophysics*, 516:A66+, June 2010.

[23] Tongyan Lin, Douglas P. Finkbeiner, and Gregory Dobler. The Electron Injection Spectrum Determined by Anomalous Excesses in Cosmic Ray, Gamma Ray, and Microwave Signals. *Phys. Rev.*, D82:023518, 2010.

[24] R. Trotta et al. Constraints on cosmic-ray propagation models from a global Bayesian analysis. *The Astrophysical Journal*, 729(2):106, 2010.

[25] D. Maurin, F. Donato, R. Taillet, and P. Salati. Cosmic Rays below Z=30 in a diffusion model: new constraints on propagation parameters. *Astrophys. J.*, 555:585–596, 2001.

[26] David Maurin, Richard Taillet, and Fiorenza Donato. New results on source and diffusion spectral features of Galactic cosmic rays: I- B/C ratio. *Astron. Astrophys.*, 394:1039–1056, 2002.

[27] D. Maurin, A. Putze, and L. Derome. Systematic uncertainties on the cosmic-ray transport parameters. Is it possible to reconcile B/C data with $\delta = 1/3$ or $\delta = 1/2$? *Astronomy and Astrophysics*, 516:A67+, June 2010.

[28] (ed.) Ginzburg, V.L., V.A. Dogiel, V.S. Berezinsky, S.V. Bulanov, and V.S. Ptuskin. *Astrophysics of cosmic rays*. North Holland, 1990.

[29] S. Gillessen, F. Eisenhauer, S. Trippe, T. Alexander, R. Genzel, et al. Monitoring stellar orbits around the Massive Black Hole in the Galactic Center. *Astrophys.J.*, 692:1075–1109, 2009.

[30] Andrew W. Strong, Igor V. Moskalenko, and Vladimir S. Ptuskin. Cosmic-ray propagation and interactions in the Galaxy. *Ann. Rev. Nucl. Part. Sci.*, 57:285–327, 2007.

[31] A.W. Strong, I.V. Moskalenko, T.A. Porter, G. Johannesson, E. Orlando, et al. The GALPROP Cosmic-Ray Propagation Code. 2009.

[32] O. Adriani et al. A statistical procedure for the identification of positrons in the PAMELA experiment. *Astropart.Phys.*, 34:1–11, 2010.

[33] O. Adriani et al. PAMELA results on the cosmic-ray antiproton flux from 60 MeV to 180 GeV in kinetic energy. *Phys. Rev. Lett.*, 105:121101, 2010.

[34] Igor V. Moskalenko, Andrew W. Strong, Jonathan F. Ormes, and Marius S. Potgieter. Secondary anti-protons and propagation of cosmic rays in the galaxy and heliosphere. *Astrophys.J.*, 565:280–296, 2002.

[35] K. E. Krombel and M. E. Wiedenbeck. Isotopic composition of cosmic-ray boron and nitrogen. *Astrophys. J.*, 328:940–953, May 1988.

[36] J. A. Lezniak and W. R. Webber. The charge composition and energy spectra of cosmic-ray nuclei from 3000 MeV per nucleon to 50 GeV per nucleon. *Astrophys. J.*, 223:676–696, July 1978.

[37] J. J. Engelmann, P. Ferrando, A. Soutoul, P. Goret, and E. Juliusson. Charge composition and energy spectra of cosmic-ray nuclei for elements from Be to NI - Results from HEAO-3-C2. *Astronomy and Astrophysics*, 233:96–111, July 1990.

[38] E. Mocchiutti et al. The PAMELA Experiment: Preliminary Results after Two Years of Data Taking. In *21st European Cosmic Ray Symposium (ECRS 2008)*, Proceeding of 21st European Cosmic Ray Symposium, pages 396–401, 2008.

[39] H. S. Ahn et al. Measurements of cosmic-ray secondary nuclei at high energies with the first flight of the CREAM balloon-borne experiment. *Astropart. Phys.*, 30:133–141, 2008.

[40] A. J. Davis, R. A. Mewaldt, W. R. Binns, E. R. Christian, A. C. Cummings, J. S. George, P. L. Hink, R. A. Leske, T. T. von Rosenvinge, M. E. Wiedenbeck, and N. E. Yanasak. On the low energy decrease in galactic cosmic ray secondary/primary ratios. In R. A. Mewaldt, J. R. Jokipii, M. A. Lee, E. Möbius, & T. H. Zurbuchen , editor, *Acceleration and Transport of Energetic Particles Observed in the Heliosphere*, volume 528 of *American Institute of Physics Conference Series*, pages 421–424, September 2000.

[41] M. Hareyama. SUB-Fe/Fe ratio obtained by Sanriku balloon experiment. In *International Cosmic Ray Conference*, volume 3 of *International Cosmic Ray Conference*, pages 105–+, August 1999.

[42] M. E. Wiedenbeck and D. E. Greiner. A cosmic-ray age based on the abundance of Be-10. *Astrophysical Journal*, 239:L139–L142, August 1980.

[43] M. Garcia-Munoz, T. G. Guzik, S. H. Margolis, J. A. Simpson, and J. P. Wefel. The Energy Dependence of Cosmic-Ray Propagation at Low Energy. In *International Cosmic Ray Conference*, volume 9 of *International Cosmic Ray Conference*, pages 195–+, 1981.

[44] T. Hams, L. M. Barbier, M. Bremerich, E. R. Christian, G. A. de Nolfo, S. Geier, H. Goebel, S. K. Gupta, M. Hof, W. Menn, R. A. Mewaldt, J. W. Mitchell, S. M. Schindler, M. Simon, and R. E. Streitmatter. ^{10}Be/^{9}Be ratio up to 1.0 GeV/nucleon measured in the ISOMAX 98 balloon flight. In *International Cosmic Ray Conference*, volume 5 of *International Cosmic Ray Conference*, pages 1655–+, August 2001.

[45] A. J. Davis, R. A. Mewaldt, W. R. Binns, E. R. Christian, A. C. Cummings, J. S. George, P. L. Hink, R. A. Leske, T. T. von Rosenvinge, M. E. Wiedenbeck, and N. E. Yanasak. On the low energy decrease in galactic cosmic ray secondary/primary ratios. *AIP Conference Proceedings*, 528(1):421–424, 2000.

[46] N. E. Yanasak, M. E. Wiedenbeck, W. R. Binns, E. R. Christian, A. C. Cummings, A. J. Davis, J. S. George, P. L. Hink, M. H. Israel, R. A. Leske, M. Lijowski, R. A. Mewaldt, E. C. Stone, and T. T. von Rosenvinge. Cosmic-ray time scales using radioactive clocks. *Advances in Space Research*, 27:727–736, 2001.

[47] J. Burger. Cosmic ray physics with AMS. *European Physical Journal C*, 33:941–943, 2004.

[48] A. S. Beach, J. J. Beatty, A. Bhattacharyya, C. Bower, S. Coutu, M. A. Duvernois, A. W. Labrador, S. McKee, S. A. Minnick, D. Müller, J. Musser, S. Nutter, M. Schubnell, S. Swordy, G. Tarlé, and A. Tomasch. Measurement of the Cosmic-Ray Antiproton-to-Proton Abundance Ratio between 4 and 50 GeV. *Physical Review Letters*, 87(26):A261101+, December 2001.

[49] J. T. Childers and M. A. Duvernois. Expected boron to carbon at TeV energies. In *International Cosmic Ray Conference*, volume 2 of *International Cosmic Ray Conference*, pages 183–186, 2008.

[50] A. G. Malinin. Astroparticle physics with AMS-02. *Phys. Atom. Nucl.*, 67:2044–2049, 2004.

[51] Timur Delahaye et al. Anti-Matter in Cosmic Rays : Backgrounds and Signals. *arXiv:0905.2144*, 2009.

[52] D. Grasso et al. On possible interpretations of the high energy electron- positron spectrum measured by the Fermi Large Area Telescope. *Astropart. Phys.*, 32:140–151, 2009.

[53] Boaz Katz, Kfir Blum, and Eli Waxman. What can we really learn from positron flux 'anomalies'? *Monthly Notices of the Royal Astronomical Society*, 405(3):1458–1472, 2009.

[54] Warrit Mitthumsiri. Cosmic-ray positron measurement with the fermi-lat using the earth's magnetic field. In *Fermi Symposium*, Fermi Symposium, May 2011.

[55] Luca Maccione, Carmelo Evoli, Daniele Gaggero, Giuseppe Di Bernardo, and Dario Grasso. DRAGON: A public code to compute the propagation of high-energy Cosmic Rays in the Galaxy., 2010.

[56] David Maurin, Antje Putze, Laurent Derome, Richard Taillet, Fernando Barao, Fiorenza Donato, Pierre Salati, and CÃl'line Combet. USINE - a galactic cosmic-ray propagation code., 2011.

[57] Marco Cirelli, Gennaro Corcella, Andi Hektor, Gert Hutsi, Mario Kadastik, et al. PPPC 4 DM ID: A Poor Particle Physicist Cookbook for Dark Matter Indirect Detection. *JCAP*, 1103:051, 2011.

[58] I. Buesching, A. Kopp, M. Pohl, and R. Shlickeiser. A New Propagation Code for Cosmic Ray Nucleons. In *International Cosmic Ray Conference*, volume 4 of *International Cosmic Ray Conference*, pages 1985–+, July 2003.

[59] Markus Ahlers, Philipp Mertsch, and Subir Sarkar. On cosmic ray acceleration in supernova remnants and the FERMI/PAMELA data. *Phys. Rev.*, D80:123017, 2009.

[60] Lars Bergstrom, Joakim Edsjo, and Gabrijela Zaharijas. Dark matter interpretation of recent electron and positron data. *Phys. Rev. Lett.*, 103:031103, 2009.

[61] Ilias Cholis, Douglas P. Finkbeiner, Lisa Goodenough, and Neal Weiner. The PAMELA Positron Excess from Annihilations into a Light Boson. *JCAP*, 0912:007, 2009.